University of Huddersfield Repository

Meriaux, J., Fouvry, S., Kubiak, Krzysztof and Deyber, S.

Characterization of crack nucleation in TA6V under fretting-fatigue loading using the potential drop technique

Original Citation

Meriaux, J., Fouvry, S., Kubiak, Krzysztof and Deyber, S. (2010) Characterization of crack nucleation in TA6V under fretting-fatigue loading using the potential drop technique. International Journal of Fatigue, 32 (10). 1658 - 1668. ISSN 0142-1123

This version is available at http://eprints.hud.ac.uk/id/eprint/21598/

http://eprints.hud.ac.uk/

Characterization of Crack Nucleation in TA6V under Fretting-Fatigue loading using the potential drop technique

J. Meriaux[1,2], S. Fouvry[1], K. Kubiak[1], S. Deyber[2]

[1] Laboratoire de Tribologie et de Dynamique des Systèmes (LTDS), Ecole Centrale Lyon, France

[2] SNECMA, Site de Villaroche, 77550 Moissy-Cramayel, France

krzysztof@kubiak.co.uk

Abstract

In this work, the crack nucleation under fretting and fretting fatigue loading was investigated experimentally on a Ti-6Al-4V alloy. The geometry considered is a cylinder on flat contact in stick slip conditions. A new dual actuator fretting fatigue device was presented and an original interrupted test expertise methodology was proposed. In order to quantify the crack nucleation, the fretting fatigue set-up was equipped with a potential drop technique device. A proper calibration, presented in this paper, allowed a crack nucleation detection threshold of 50 μm with an error threshold of 10% at the maximum. Three parallel studies have been carried out: fretting loading tests (optical expertise), fretting fatigue test for a lifetime of 100 000 (optical expertise) and fretting fatigue interrupted tests (potential drop technique). These tests have shown that the addition of a fatigue load can provide a fall of 45% of the tangential threshold of crack nucleation compared to simple fretting loading. It has been identified that the crack nucleation is influenced by the fretting and the fatigue forces in two ways: increasing the fatigue load leads to a decrease of the tangential force nucleation threshold whereas raising the fretting load leads to a decrease of the nucleation and fracture fatigue lifetime. All tests curried out with the potential drop technique system have shown that this technique is very efficient in the case of a fretting fatigue test.

Keywords: fretting fatigue, crack nucleation, Ti-6Al-4V, potential drop technique

Nomenclature

R_a roughness (μm),

d   cylindrical sample radius (mm),

V   electrical potential at the edge of the crack (V),

V_0 electrical potential measured at the beginning of the test (V),

a   crack length (µm),

W   sample depth (mm),

N   number of cycles

p_o maximal Hertzian pressure in the contact (MPa),

P   normal force (N),

δ   sliding amplitude (µm),

Q   tangential load (N),

Qc   critical tangential load (N): tangential load that leads to crack nucleation for a given N

σ_{fat} fatigue load (MPa),

R   stress ratio,

N_0, N_f cycle limits used to determined the value of V_0,

µ   coefficient of friction,

a_{ref} confidential crack length that corresponds to the definition of the crack nucleation ($50\mu m < a_{ref} < 100\mu m$). This crack length is used to compare the different loading configurations.

1   Introduction

Fretting fatigue is a critical solicitation that appears on many structures such as the blade/disk contact of aircraft engines (Figure 1). It is characterized by small displacements between two bodies, one of which has an applied bulk stress. This phenomenon has been studied for a long time [1] and induces damage and eventually reduces fatigue resistance. Fretting leads to premature crack nucleation compared to classic fatigue loading.
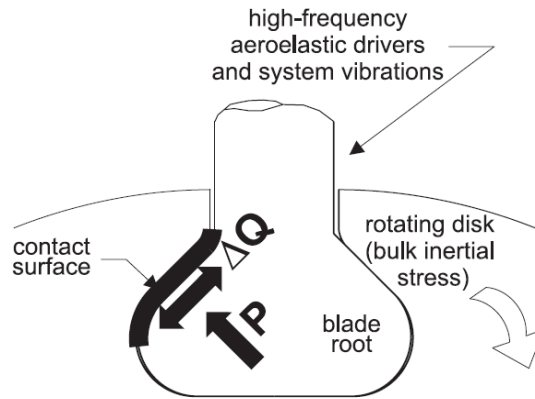
Figure 1: Illustration of the typical fretting fatigue contact configuration present at the dovetail notch of blade disk components in rotating aircraft engines [2].

The fretting fatigue damage is mainly controlled by the sliding condition. A gross slip condition associated to large sliding amplitude will lead to wear debris formation and third body ejection. Energy description of wear mechanisms has been developed in several studies [3]. On the other hand, a partial slip condition will principally induce mode II fatigue crack nucleation.

In the last decade, the effects of several parameters on the fretting fatigue behaviour have been investigated for instance the stress gradient [4, 5], the sliding regime [6], the roughness [7], the residual stresses [8], the microstructure [9, 10] and one of the main factors: the competition between the fretting and the fatigue loads [11]. In general, the influence of those parameters is studied with regards to the specimen lifetime, crack nucleation models or a combination of both: the numerical model is providing the number of cycles to nucleation. It is also possible to estimate the total life time by fracture mechanics analogy.

The total fretting fatigue life is often considered as the sum of a fretting crack nucleation and fatigue crack propagation. In those cases, the number of cycles until nucleation can be found either through performing a simulation or by using experimental detection techniques which are actually very limited. Many studies have been carried out in order to optimize the prediction of fretting and fretting fatigue cracks' nucleation. Most of them use a critical plan approach such as the SWT criterion [12-14], the Dang Van or the Ruiz parameter [15], the short crack approach[XX], etc… However, those numerical methods induce new varying parameters such as the critical volume. The influence of the number of cycles to nucleation on the total lifetime has already been studied, yet there is a lack of experimental data that can be used to quantify the crack nucleation. This data deficiency is one of the primary weaknesses in the current models [16]. Experimental data of crack nucleation is also very important in

order to validate the numerical models. Until now, many different techniques have been investigated with limited success. The most efficient technique is to correlate surface profilometry measurement with reduction in fatigue strength [17-19]. An other leading technique uses fractography and SEM observations combined with fatigue striations analysis [20]. This last technique allows access to the crack propagation kinetic and analysis of the crack initiation behaviour, but the crack nucleation analysis threshold is limited to 130 µm which corresponds to the appearance of fatigue striations.

In this study, we have investigated the general behaviour of Ti-6Al-4V material under fretting fatigue solicitation in a (P,Q,N) representation [12, 21] .We have developed a specific dual-actuator fatigue set-up capable of separately applying the fatigue and the fretting load. This experiment has been equipped with a potential drop technique device in order to precisely detect and quantify the crack nucleation and propagation. Using a particular calibration, it has been possible to look at the influence of several parameters in the nucleation life and on total life.

2   Experimental Conditions

2.1   *Material and Contact Parameters*

The material used for fretting samples, fretting fatigue samples and pads is an alpha/beta alloy (Ti-6Al-4V) commonly used in aeronautics (Figure 2). The mechanical properties are shown in Table 1. A single type of contact has been investigated using controlled roughness ($R_a = 0.5$ µm) specimens in a cylinder on plane geometry with a constant radius d = 40 mm and a constant width perpendicular to the sliding direction (plane strain conditions). The maximum compression stress (Hertzian's contact pressure) at the surface was kept constant for all tests. The working frequency is equal to 10 Hz, limited by the actuator efficiency, but no major effect of the frequency has been observed in past studies [20].
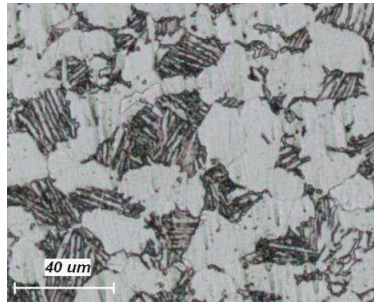
Figure 2: Duplex microstructure of Ti-6Al-4V showing alpha grains and alpha-beta lamellar structures.

Mechanical properties of Ti-6Al-4V

Elastic modulus (GPa)	119
Poisson ratio	0.29
Yield stress (MPa)	970
Density (g/cm^3)	4.4
Vickers hardness (HV$_{0.3}$)	360

Table 1: Mechanical properties of Ti-6Al-4V: data provided by SNECMA company.

2.2 Fretting Experimental Set-up

Several tests have been performed with a simple fretting load under small sliding condition in order to characterize crack nucleation without any fatigue loading. Those tests have been carried out using an experimental layout specially designed at LTDS (Figure 3); further details of this set-up can be found in [14]. A constant normal force P is applied followed by a cyclic sinusoidal displacement δ in order to generate an alternative cycle tangential load Q on the contact surface. During the tests, P, Q and δ are recorded. The sliding transition conditions have been determined through variable displacement method described in details in [14].
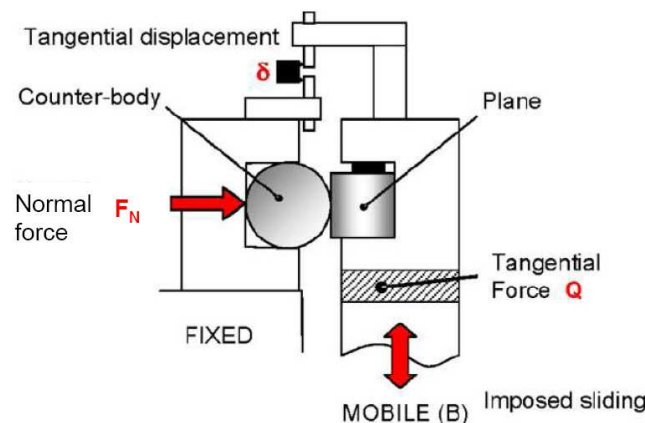
Figure 3: Schematic diagram of the LTDS fretting system for the cylinder on plane configuration.

2.3 Fretting Fatigue Experimental Set-up

A new fretting fatigue experimental set-up has been developed at LTDS (Figure 4). It was inspired by the experimental set-ups developed by Hills et al. [22] and the one developed by Mall et al. [6]. It is a dual actuator device that allows the separate application of the fretting condition and the fatigue load. Multiple sensors allow the following parameters to be recorded during tests: the fretting and the fatigue load (Q and σ_{fat}), the fretting and fatigue displacements (δ and δ_{fat}), and the fretting normal load (P). Relative displacement in the contact is measured by a contact less optical sensor installed on the fretting pad clamp and a reflecting mirror fixed on the flank of the fatigue specimen at the contact position level. The original feature of the LTDS set-up is its ability to perform single contact fretting fatigue tests due to a ball bearing located in the face opposite the contact. This system enables the application of a large diversity of combined loadings. The two main types of loading configurations are: the 'in phase' fretting fatigue loading (Figure 4 (c)) and the loading combination more representative of the real 'in flight' configuration where a cyclic plateau of bulk stress loading is combined with sinusoidal tangential fretting force (Figure 4 (d)). The experiments discussed in this paper relate only to the 'in phase' loading.
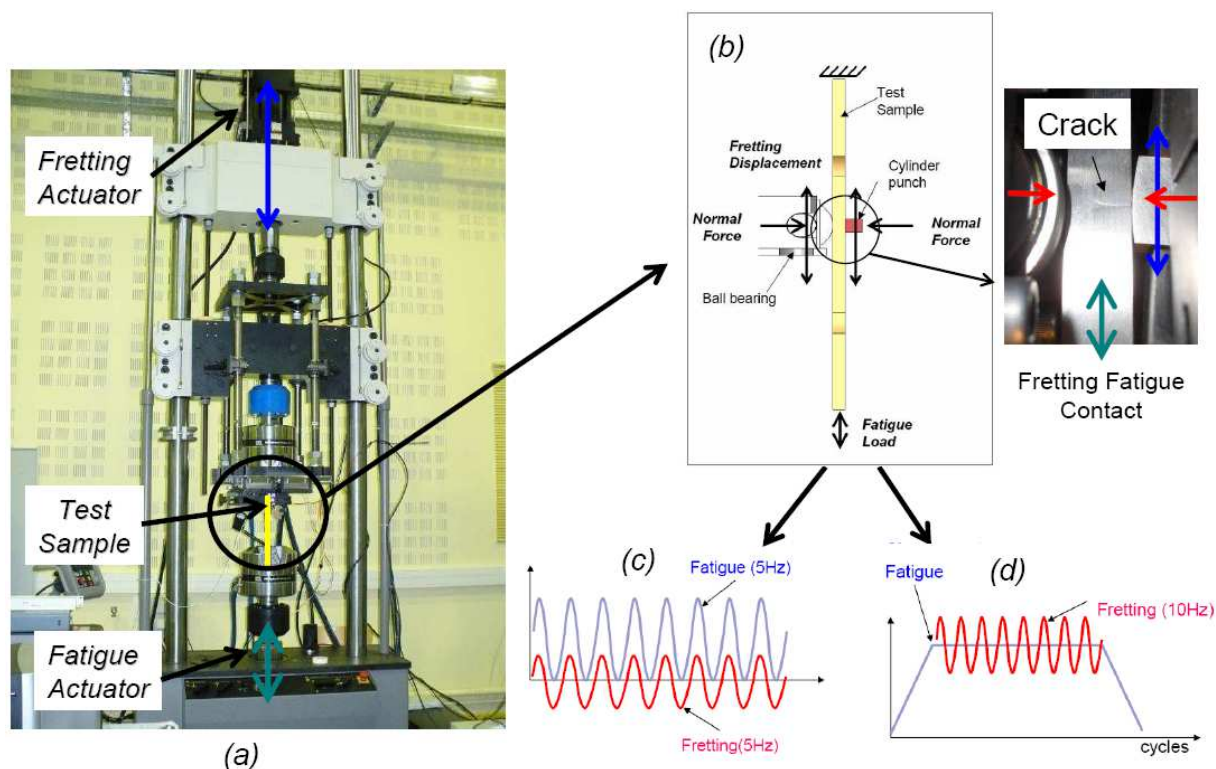
Figure 4: (a) Representation of the LTDS fretting fatigue set-up, (b) close up of the fretting contact; and the two types of classical configurations: (c) in phase and (d) cyclic constant bulk stress.

2.4   Post-test Analysis Methodology

Most of the tests presented here have been interrupted and analysed. Analyses consist of an optical determination of the crack length. The crack analysis technique has been inspired by Proudhon et al. [12]. For all fretting tests, the sample is cut in the middle of the scars. Then, the new surface created is polished and observed with an optical microscope. The polishing and observation phase is repeated triple in order to evaluate the homogeneity of the crack length. The scale of crack length studied here (0 to 80 μm) corresponds to a homogeneous mode II crack propagation in the material. Therefore, the technique used is sufficient for obtaining proper quantification of crack length.

Regarding the fretting fatigue test, the level of crack length is much higher (50 μm to 1mm) and the assessments have shown more inhomogeneous cracks. That is why the observations were taken from ten polishing planes instead of three and a chemical etching with Keller reactant was carried out on all observed planes (Figure 5).
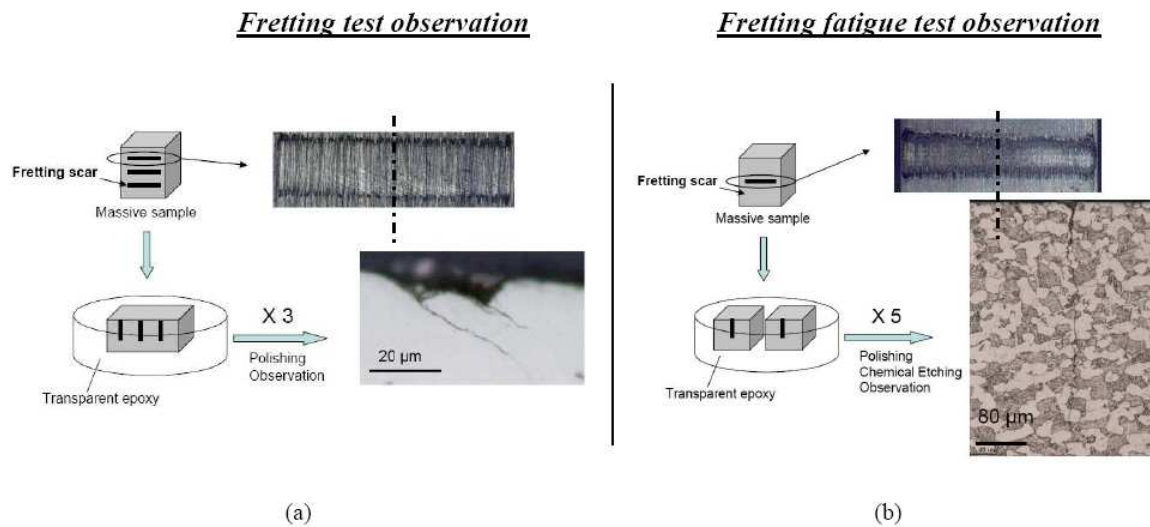
Figure 5: Experimental method to investigate cracking after fretting test (a) and fretting fatigue test (b).

2.5   Fretting Fatigue Map of Ti-6Al-4V for a Lifetime of 100 000 Cycles

Before studying the general crack nucleation of the Ti-6Al-4V/Ti-6Al-4V cylinder on plane contact, the global behaviour of this contact under a fretting fatigue loading is determined. Hence, a general (Q, σ_{fat}, N) map [21] at a specific N = 100 000 cycles (Figure 6) was designed upon. This life time was chosen because it represents HCF with acceptable test duration. Several tests were performed in order to identify the fretting and fatigue conditions that lead to failure or to crack nucleation. The cracks observed were small cracks (< 50 μm), so the fretting assessment methodology was used. The starting point of the boundary between the 'no-nucleation area' and the 'crack initiation' area (σ_{fat} = 0 MPa) was determined in the simple-fretting study.
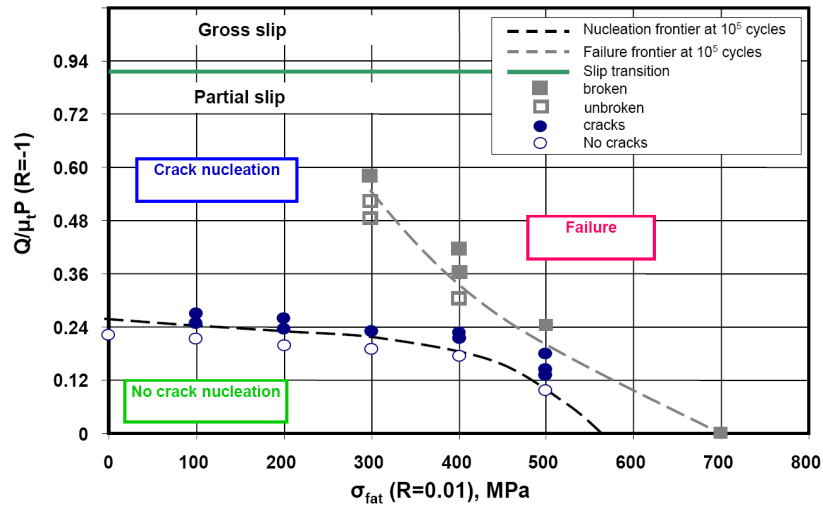
Figure 6: Fretting Fatigue Map of Ti-6Al-4V at 10^5 Cycles: Cylinder on Flat Contact.

This first study reveals very interesting results. First of all, this map allows the final state of the sample to be characterized in terms of fretting and fatigue loading in one of three ways: no crack nucleation, crack nucleation and failure. In essence, it determines a safe zone for the material. The map shows that at a lifetime equal to 10^5 cycles, there is very little influence of the fatigue force on the crack nucleation below $\sigma_{fat} = 300$ MPa. When σ_{fat} is larger than 300 MPa, the crack nucleation process is equivalently controlled by the two parameters. Concerning the failure of the sample, there is an equal effect of the two loadings.

3   Potential Drop Technique (PDT) Calibration

In order to detect the crack nucleation and quantify the crack propagation, the fretting fatigue set-up was equipped with a specific potential drop technique device. Considering the configuration of the fretting fatigue test, this method is more suitable than the classic optical or compliance methods. The idea of applying the PDT on a fretting fatigue device was first introduced by Kondo and Kubota et al. [23] and then used in their following studies [24-26]. The PDT was used on a bending fretting fatigue device. This paper completes the work of Kubota by applying the PDT in a dual actuator fretting fatigue set-up and by analysing the accuracy of the technique. This critical analysis is presented in section 3.1.

3.1   Principle of the Potential Drop Technique

This technique relies on the fact that the potential distribution in the vicinity of a crack changes with crack growth. Technique was first introduced in 1957 by W.J. Barnett and A.R. Troiano. The technique has been widely used and the calibration procedure is well known [27]. The principle is to apply plateaus of current in the specimen and to measure the difference of potential on each side of the crack. In fretting fatigue the crack nucleation appears at the edge of the contact (see Figure 7).
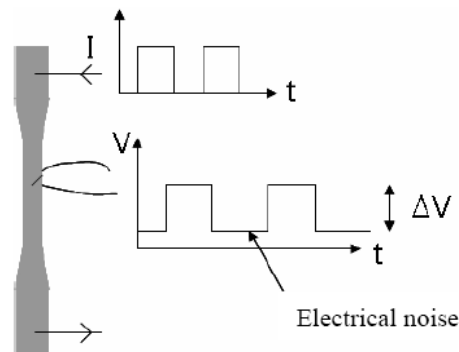

Figure 7: Schematic diagram of the Potential Drop Technique Principle.

The propagation of the crack induces a diminution of the sample cross section that leads to an increasing of the electrical resistance. As the intensity of the current is constant, an increase in the electrical resistance is directly connected with an increase of the electrical potential. By monitoring this increase, V, and comparing it with the reference value V_0 measured at the beginning of the test, the average crack depth (a), or the crack depth ratio (a/W) can be determined, where W is the depth of the sample. A calibration curve is thus useful in converting the potential measurements into crack lengths. For a given configuration, calibration consists in finding the solutions to Laplace's equation (eq. 1) within the boundary conditions of particular test piece geometry.

$$\nabla^2 (V) = 0 \qquad \text{eq. 1}$$

There are three main ways to determine the calibration curve for a specific test configuration: analytical methods, numerical methods, and empirical methods. Analytical solutions have many advantages and solutions of Laplace's equation have already been obtained for simple geometries [27]. In fact, there are many analytical solutions corresponding to all classical fatigue sample geometries [28]. Unfortunately, in fretting fatigue test, no standard on the test specimen has been determined and no study on calibration curves has been carried out.

Moreover, most of the classical geometries concern pre-cracked sample, which is not the case of our investigation.

The numerical calibration by using the 2-D or 3-D finite element method also offers multiple advantages and has been used in many cases for fatigue tests with particular geometries or loading conditions [29-31]. This method, however, is not adapted to our testing conditions due to the contact configuration where the fretting pad conducts part of the current. Therefore, the solution that has been used to obtain the calibration is the empirical method, which consists in an experimental description of the calibration curve. This calibration was also used by Kondo and Kubota [23], but not fully described in paper.

3.2 Calibration Methodology

The most important point is to establish the repeatability of the experiment method. The installation of the electrical set-up is identical for all tests and the determination of the V_0 is calculated as follow:

$$V_0 \Rightarrow \min_{N_f - N_0 = 4000} \left\{ \sum_{N_i = N_0}^{N_f} \frac{V(N_i) - V_0}{V_0} \right\} \qquad \text{eq. 2}$$
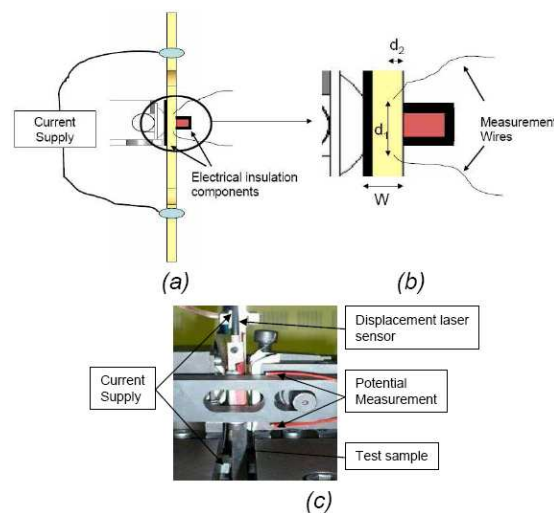

Figure 8: Schematic of the experimental set-up: (a) positioning of the current supply and isolation, (b) positioning of the measurement wires, (c) picture of the experimental set-up.

The technique implies a complete insulation of the system {sample + pad}. So insulating components are placed between both the sample and the ball bearing and between the pad and the fretting set-up (Figure 8). Insulation of the specimen from the machine is not necessary.

11

The positioning of the measurement wires has been optimised (d_1,d_2: Figure 8) in order to obtain noise less potential measurements. D_1 must be very small to have a good signal but large enough to be sure that the crack is located between the two wires. The wires are welded on samples with a specific 'spot welding' device. Even if the test sample is not pre-cracked, the fretting fatigue configuration, determine the crack initiation to be placed under the edge of the contact area. The welding process generates an insignificant flaw compared to the contact gradient influence in terms of crack nucleation.

The objective of conducting the empirical calibration is to perform a number of tests, thereby obtaining experimental values of {a/W, V/V_0} points. Then, several polynomial functions are used to correlate those experimental points. In order to optimise the calibration, two methodologies have been used:

- Small cracks (< 600 μm): V_0 is evaluated at the beginning of the test. Then the test is interrupted at a specific value of V/V_0 and the sample is optically observed following the methodology illustrated in Figure 5 (b). The values of V/V_0 were between 1,005 (Figure 9 (a)) and 1,062 and corresponded to 50 μm - 596 μm cracks.

- Large cracks (> 600 μm): V_0 is evaluated at the beginning of the test. Then the load ratio is modified alternatively from 0.01 to 0.5 and from 0.5 to 0.01 in order to obtain different fracture morphologies in fracture plane on the same sample. The area of successive morphologies are measured from optical microscope images, then divided by the contact width to obtain an average crack length (Figure 9). If the differences of fracture surface are not notable enough, a heating treatment is applied in order to diversify them.
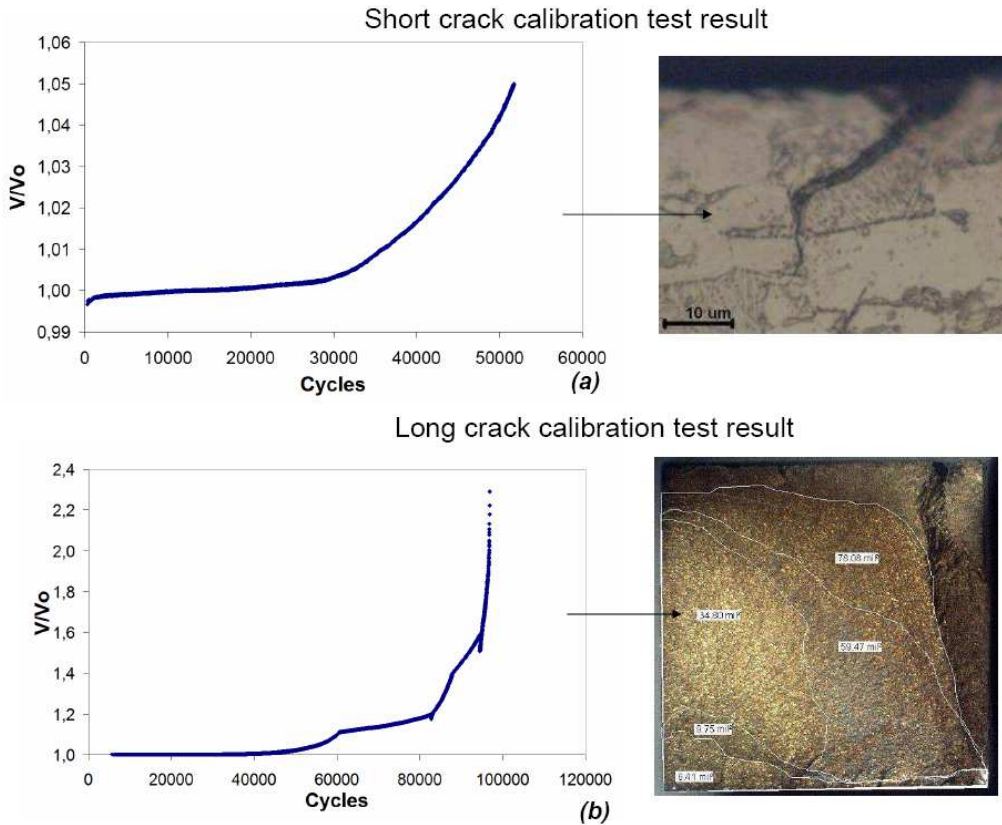
Figure 9: (a) Typical curve V = f(N): test stopped at $V/V_0 = 1,05$, $\sigma_{fat} = 400$ MPa and $Q^*/\mu_t P$ = +/- 0.29 and corresponding observation, (b) Typical curve V = f(N) for a long crack calibration test: $\sigma_{fat} = 400$ MPa with four conditions changes during one test and corresponding observations.

3.3 Definitive Calibration

Nine calibration tests were carried out in present study: six for short cracks and three for long cracks. From both analysis methodologies, we obtain a good general view of the crack geometry. One observation is that for a crack over 100 μm, the propagation can be very inhomogeneous. This will be a significant issue because measurement wires are welded on only one face of the sample. An analysis of the accuracy of the calibration is presented below. Sufficient information has been obtained in order to find a correct calibration curve. Three polynomial functions have been used with three different values for each coefficient depending on the value of V/V0:

$$\frac{a}{W} = A_1\left(\frac{V}{V_0}\right)^5 + A_2\left(\frac{V}{V_0}\right)^4 + A_3\left(\frac{V}{V_0}\right)^3 + A_4\left(\frac{V}{V_0}\right)^2 + A_5\left(\frac{V}{V_0}\right)^1 + A_6 \quad \text{eq. 3}$$

Due to industrial character of presented study the values of the coefficients A_1 - A_5 are confidential.
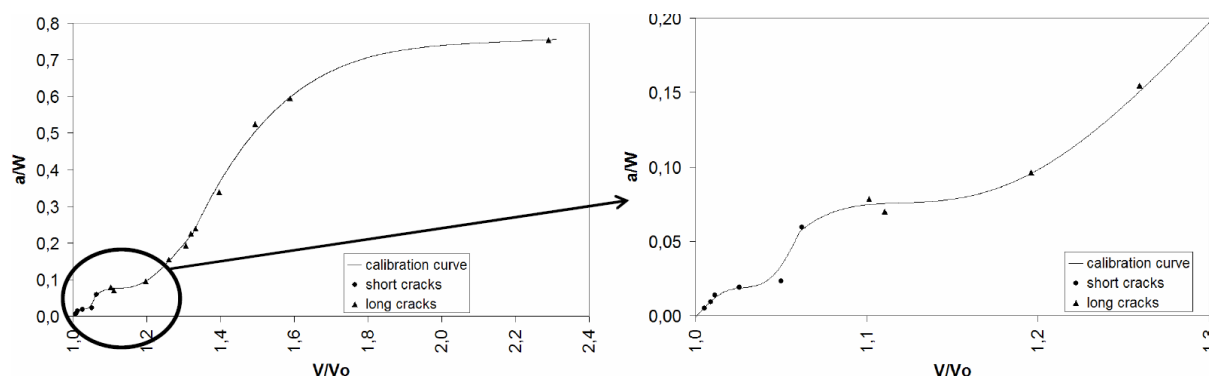

Figure 10: Fretting-fatigue Potential Drop Technique, empirical calibration curve for a cylinder on flat contact configuration, close-up for short cracks analysis.

Several interesting points can be noted on Figure 10. First of all, with the proposed methodology, it is possible to obtain a crack nucleation detection threshold at vary small level of 50 μm which corresponds to a very short crack. It is important to note that SEM observations of fracture surface have shown that the pure mode II propagation corresponds to 50 μm to 100 μm cracks. Therefore, the detection threshold corresponds either to a pure mode II crack or to the boundary between pure mode II and mixed mode I-mode II crack propagation. It is also notable that the calibration curve presents two plateaus: one at a/W = 0.02 and the other at a/W = 0.08 (Figure 10). A plateau corresponds to a large augmentation of the measured resistance at a stable value of a/W. So those plateaus correspond to a large opening of the crack without propagation which means that it corresponds to transitions of the propagation process (mode II to mode I/mode II to mode I). The transition from a pure mode II propagation to a mode I/mode II propagation creates a crack opening that induces an increase in the electrical potential. This phenomenon is also related to the way the crack length is determined. The small crack length is evaluated without distinction between an open and a closed area: only the global length is being considered. It is also important to notice that the shape of the calibration curve is very different from the curve obtained by Kondo [23]. This shows that the calibration curve shape is extremely dependent of the loading configuration and of the methodology used to obtain it (crack length measurement methodology …).
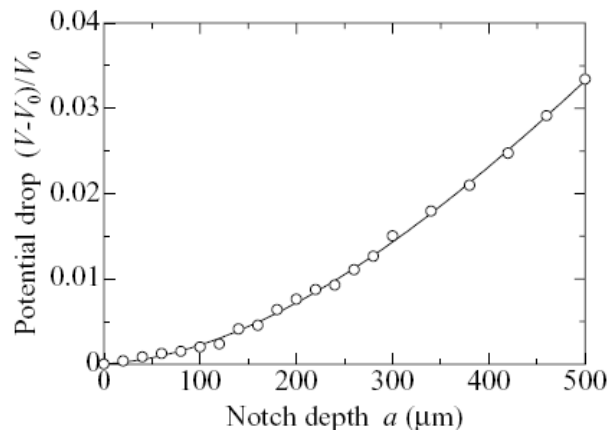
Figure 11: Calibration Curve between Potential drop and notch depth obtained by Kondo et al. [23].

4 Fretting Results: Characterisation of Crack Nucleation under simple fretting loading (without Fatigue Load)

The first step in the characterization of the crack nucleation is to observe the crack behaviour without the fatigue load. In this scenario, the contact configuration is fixed and the only varying parameter is the tangential force amplitude. We characterize the crack nucleation following the methodology introduced by Proudhon et al. [12]. First, the value of P is imposed. Then, for different values of N, we perform several tests at different tangential load values in order to find the correct crack nucleation threshold Q_c.

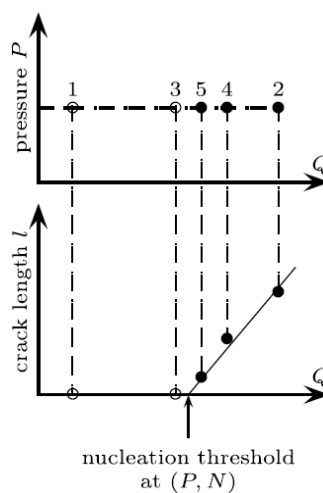Each test has been analyzed following the methodology described in section 2.4 (Figure 5a).

Figure 12: Methodology used to determine the crack nucleation threshold with respect to Q,N parameters (P and N are constant) [12].
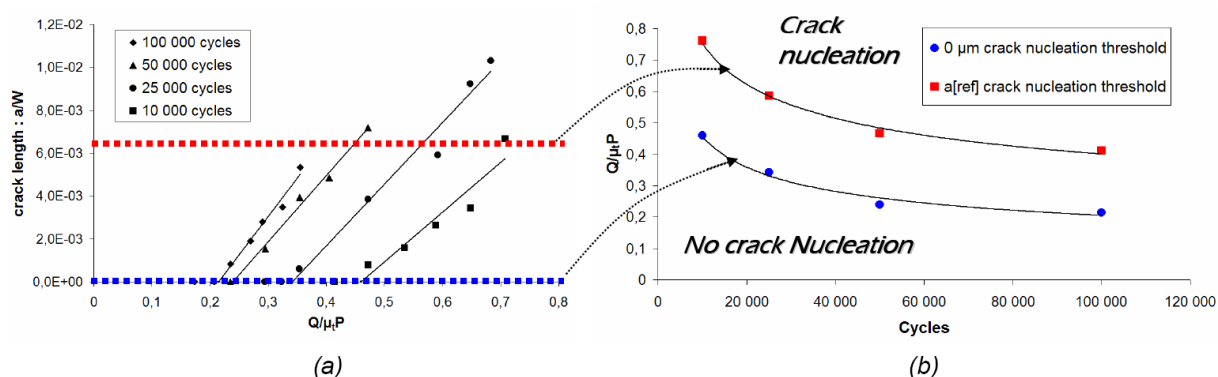
Figure 13: (a) Experimental results of crack length observed at a specific {Q,N} value, (b) Evolution of the critical tangential force Q_c to initiate fretting cracks (0 µm cracks or a_{ref} cracks) in relation to the number of cycles.

The number of applied fretting cycles has a major influence on Q_c. As observed in [12], the evolution of $Q_c(N)$ shows a rapid decrease then tends to a saturation value. This methodology allows to determine the evolution of the crack nucleation threshold for different crack lengths. The Figure 13 (b) shows the evolutions of the crack nucleation threshold for a=0 µm crack and for the a_{ref} crack (confidential value between 50 and 100 µm). Value of a_{ref} corresponds to our reference crack whose length is still in a pure mode II propagation (either in fretting or in fretting fatigue for our configuration). Crack length a_{ref} is a small crack however, is measurable in both simple fretting and fretting fatigue tests. Hence, a_{ref} is our reference value to compare fretting and fretting fatigue results. Further, a_{ref} is assumed to be the transitional length of crack between pure mode II propagation and mixed mode propagation. We have now determined the correct tangential load nucleation threshold that identifies the 'no crack nucleation' area (the curve in Figure 13b).

5   Fretting Fatigue Results

During the study of the crack nucleation, two fatigue levels and their respective five levels of fretting conditions were considered. All the tests were interrupted at V/V0 ~ 1,06 and analysed following the procedure described in section 2.4 (Figure 5b).

5.1   *Investigation on the Potential Drop Technique efficiency*

The test results were plotted on the calibration curve in order to evaluate the precision of the measurement: Figure 14.
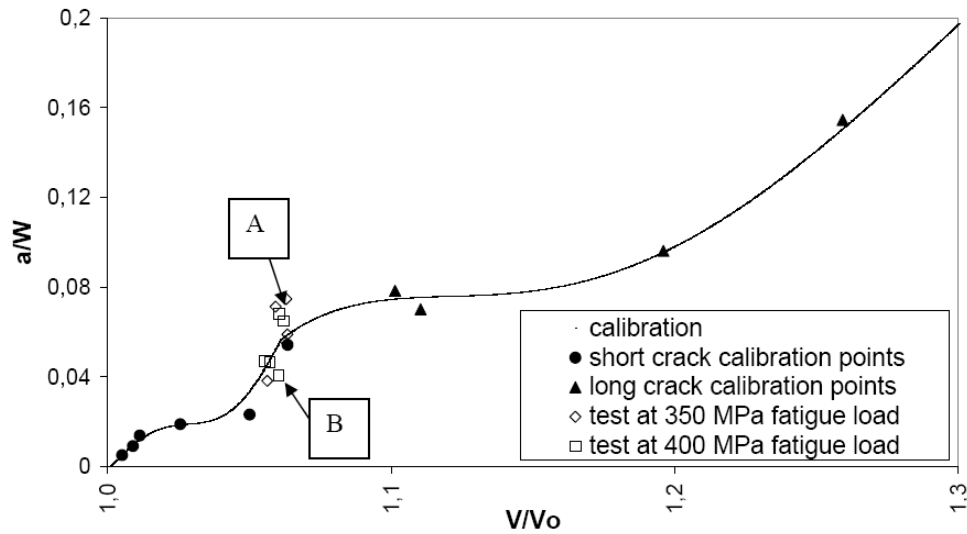

Figure 14: Positioning of the expertises of fretting fatigue tests on the potential drop technique calibration curve.

Out of eleven tests, eight experimental points are closer than 15% to the calibration curve, and six of these are closer than 10%. However, several fretting fatigue tests seem to be quite far from the prediction of the potential drop technique. The points A and B on Figure 14 have a gap of approximately 20 to 25 % from the calibration curve. If we take closer look at tests A and B (Figure 15) we can see that in each of the two cases the cracks have initiated and propagated in a corner of contact. This explains the gaps, which were observed:

- Test A: the cracks have initiated and propagated in the opposite corner from the measurement wires. Hence, for a specific value of V/V_0 the crack is in fact longer than expected because the quality of detection is less efficient.

- Test B: the cracks have initiated and propagated in the corner between the two measurement wires. Therefore, the detection is acute and for a specific value of V/V_0, the crack is shorter than expected.

This phenomenon has been observed for all tests, which presented a big difference between the experimental crack length measured and the calibration curve. For all of these tests, the optical analyses have confirmed a corner crack nucleation and propagation.
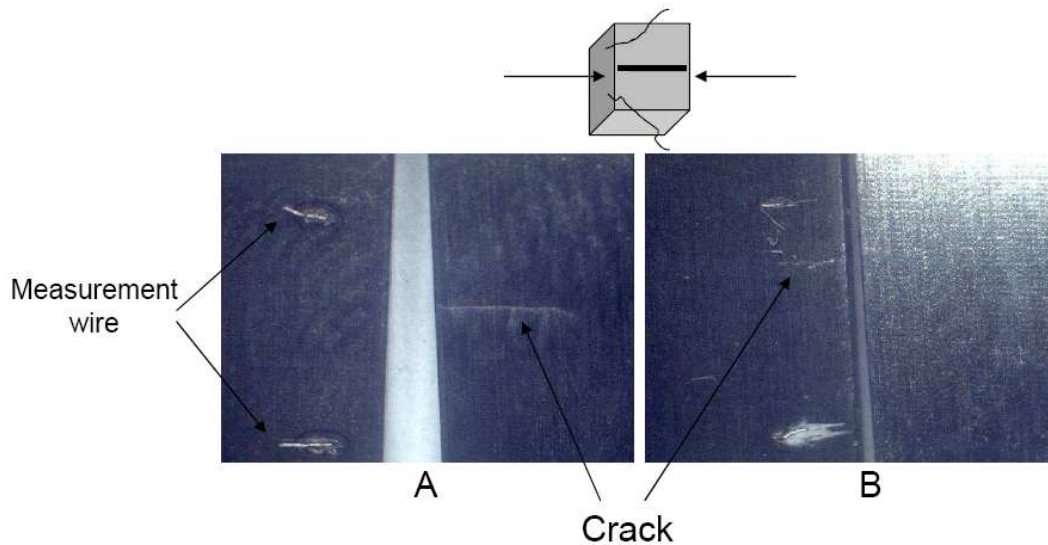
Figure 15: Pictures of the two sides of sample A and B: position of the cracks with respect to the measurement wires.

It could be conclude thant proposed technique is very efficient, but in the case of corner cracks, a correction is needed. This problem comes from the fact that the acquisition system contains only one measurement circuit line.

Now the technique can be optimised, however, as an optical analysis allows us to adjust the calibration curve according to the precise test. A homothety transformation is thus applied to the coefficients of the polynomial function (Figure 16). Considering a rupture of sample, a quick optical analysis permits to determine if the crack has propagated in a corner, and if so, how to optimise the calibration by choosing the A or the B fitted curve. The decrease in efficiency due to a corner crack on the opposite side of the measurement wire leads to the crack nucleation detection threshold decreasing to 66 μm. Assuming this we consider the threshold to be determined by $V/V_0 = 1,005$ and that the worst case calibration curve is the A curve. in this way, the technique of fitting the curve is validated (the crack nucleation and propagation processes are always the same) and that the reference calibration curve is correct. Therefore, the threshold is fixed by a crack length of 50 μm (that has been obtained during the calibration work) after fitting the calibration curve to the specific test.
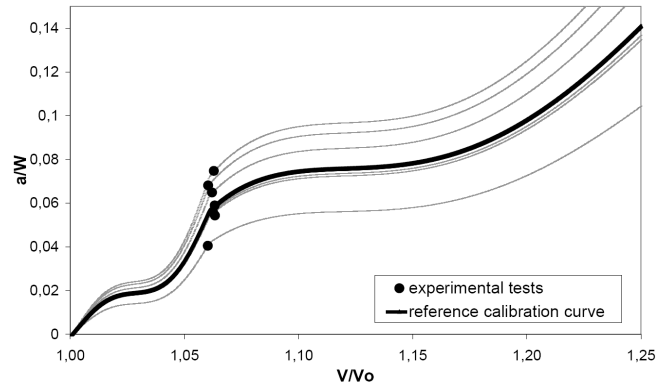
Figure 16: Process of fitting calibration curve for various fretting fatigue tests.

5.2   Fretting Fatigue Crack Nucleation Analysis

Two levels of fatigue load have been studied, as well as the case without any fatigue load (simple fretting tests). Five values of fretting loadings have been applied for each fatigue condition. The Figure 17 illustrates the evolution of potential ratio V/V_0 and the corresponding crack evolution for all tests. Cracks lengths have been calculated using the fitted calibration curve for each test.
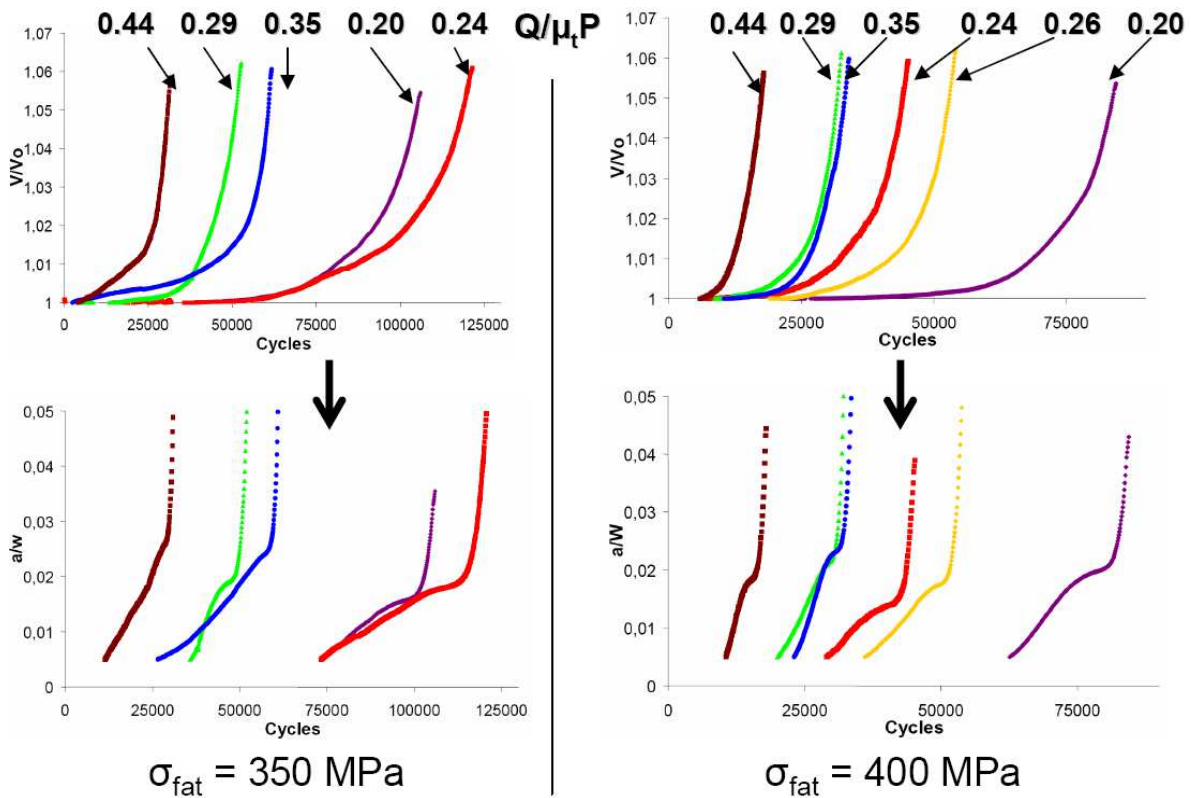
Figure 17: Evolution of V/Vo for all fretting fatigue tests and the corresponding crack length evolutions.

Figure 17 is rich in information; it shows the same curve shape for all tests, thereby validating the fact that all the tests are reproductive. There are clearly two phases in propagation which can be identified by the change of the curve's slope. This behaviour swing appears for crack lengths between 150 μm and 250 μm. We can also see a general trend that when the tangential load increases, the number of cycles to nucleate cracks is decreasing. The Figure 17 shows occasional deviation from this trend, but this can be related to general fatigue dispersion. We can now observe the influence of the fatigue loading. The Figure 18 presents the influence of the fatigue force on the nucleation of the a_{ref} crack. It can be noted that the fatigue loading has a significant influence on the crack nucleation with a $Qc/\mu_t P$ threshold reduction of 45 % compared to the simple fretting loading threshold. Thus, we cannot assume that in fretting fatigue the crack nucleation is only controlled by the tangential loading reaching a certain value of fretting load. It also appears that an increase of the fatigue load leads to a decrease of the tangential force threshold.
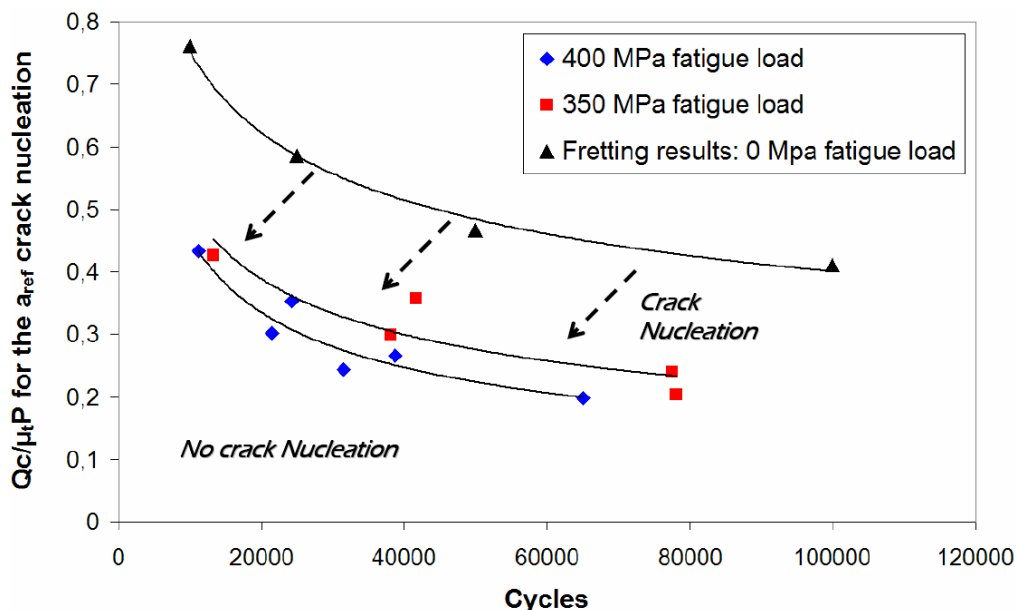

Figure 18: Tangential load threshold as a function of the number of cycle until obtaining the a_{ref} crack for fretting fatigue solicitation: influence of the fatigue load.

The crack propagation "following device" gives access to information at every crack length. This means that using proposed methodology it is possible to follow the evolution of the crack

propagation under fretting and fretting fatigue loadings. One application is to optimize the approach of the experiment. Figure 19 leads to admit that at a certain crack length (a/W = 0.04) the sample can be considered as fractured because the $Qc/\mu_t P = f(N)$ curves are almost superimposed. The tests can therefore be interrupted at a/W = 0.04 for analysis with the test time still considered to be the total life time.
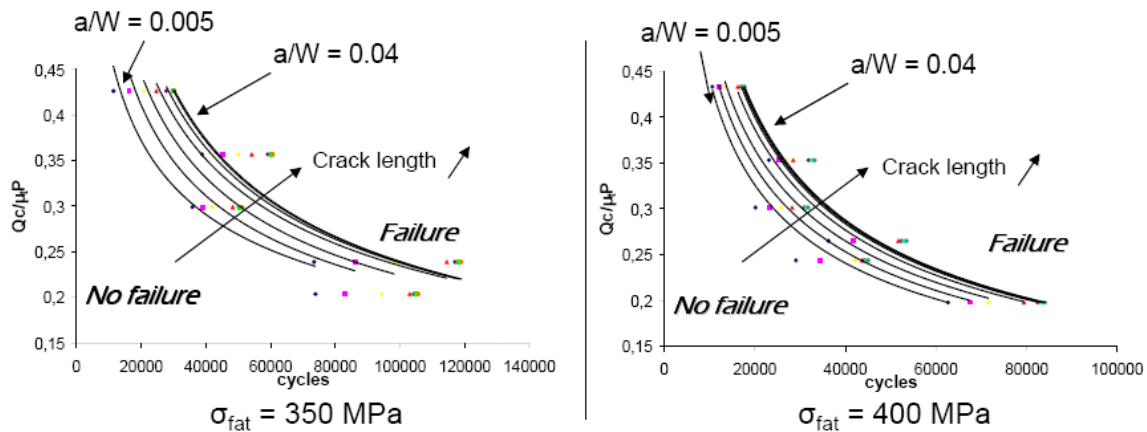

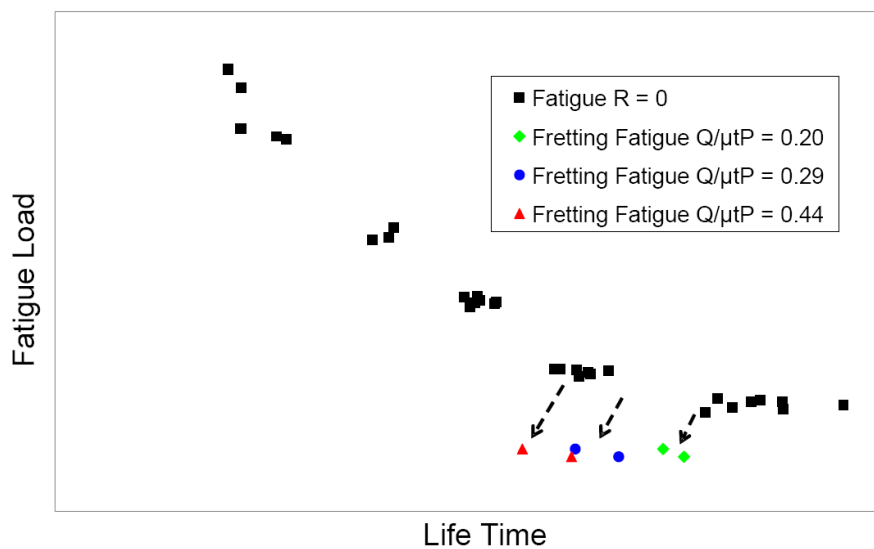Figure 19: Evolution of the tangential crack nucleation threshold for different crack lengths.

Figure 20: Fatigue Whöler curve: Positioning of Fretting Fatigue lifetime results: life time drop observation (the stress values are confidential).

We can accept that the interrupted test duration time corresponds to the total lifetime of the specimen. Figure 20 shows the life time drop due to fretting fatigue. This drop can be from 30% to 60% of the initial life time for pure fatigue. Further, we can assume that this lifetime drop is due to the fretting contact load that initiates premature cracks. This happens in two

ways: the crack nucleation is accelerated more by the tangential force than by the fatigue load, and the crack propagation is accelerated more by the fatigue force than by the simple fretting load. These results confirm what we have shown in Figure 6. Considering the level of fatigue loading, we have seen in both studies that there is a significant influence of both forces: fretting and fatigue.

6   Conclusions

Two crack nucleation approaches have been presented: optical analysis and potential drop technique (PDT). The first breakthrough presented in this paper is the use of the potential drop technique on a dual actuator fretting fatigue set-up (fretting fatigue in traction). This paper presents the calibration methodology that led to a crack nucleation detection threshold of 50 μm. The PDT precision was tested and we have shown that the optimization of the data treatment can lead to a calibration margin of error below 10%. using proposed methodology it is possible to detect a 50 μm crack and to measure its propagation rate quantitatively up to failure of specimen.

Three separate studies were carried out:

- a fretting study which resulted in fast quantification of crack nucleation under simple fretting load,
- the first representation of the crack nucleation-propagation behaviour of Ti-6Al-4V, illustrated by a fretting fatigue map (Q, σ) at 100 000 cycles, and
- a fretting fatigue study equipped with a potential drop technique which allowed to precisely quantify the crack nucleation threshold (Q_c). We have shown that the crack nucleation is not only driven by the fretting loading but also by the fatigue force in our test configuration.

The potential drop technique also demonstrates a change in the crack propagation behaviour. Two propagation behaviours have been observed in a range of crack lengths corresponding to a mode I-mode II propagation. Complementary observations are in progress, with the dual goal of optimising the quantification of the crack propagation and of linking the quantitative information to a qualitative explanation of the crack propagation behaviour. Other test configurations, conditions and loadings will be studied with the potential drop equipment to complete knowledge of the influence of each parameter on the crack nucleation behaviour.

Acknowledgements

References

1. D.W. Hoeppner, V. Chandrasekaran, C.B. Elliot, Fretting-fatigue: current technologies and practices. ASTM. 2000. STP 1367

2. M.P. Szolwinski, J.F. Matlik, T.N. Farris, Effects of HCF loading on fretting fatigue crack nucleation. International Journal of Fatigue. 1999. 21

3. S. Fouvry, T. Liskiewicz, Ph. Kapsa, S. Hannel, E. Sauger, An energy description of wear mechanism, and its application to oscillating sliding contacts. WEAR. 2003. 255

4. S. Fouvry, P. Kapsa, L. Vincent, A multiaxial fatigue analysis of fretting contact taking into account the size effect. Fretting Fatigue: current technology an practices, ASTM STP 1367. 2000

5. D. Nowell, D. Dini, Stress gradient effects in fretting fatigue. Tribology international. 2003. 36

6. H. Lee, S. Mall, Investigation into effects and interaction of various fretting fatigue varaibles under slip-controlled mode. Tribology international. 2006. 39

7. H. Proudhon, S. Fouvry, J-Y. Buffière, A fretting crack initiation prediction taking into account the surface rougness and the crack nucleation process volume. International Journal of Fatigue. 2005. 27

8. S.A. Martinez, S. Sathish, M.P. Blodgett, S. Mall, S. Namjoshi, Effects of fretting fatigue on the residual stress of shot peened Ti-6Al-4V samples. Materials science & engineering. 2005. A 399

9. S. Mall, S.A. Namjoshi, W.J. Porter, Effects of microstructure on fretting fatigue crack initiation behavior of Ti-6Al-4V. Materials science & engineering. 2004. A 383

10. T.A. Venkatesh, B.P. Conner, C.S. Lee, A.E. Giannakopoulos, T.C. Lindley, S. Suresh, An Experimental Investigation of Fretting Fatigue in Ti-6Al-4V: the Role of

Contact Conditions and Microstructure. Metallurgical and Materials Transactions. 2001. 32A

11.   S.A. Namjoshi, S. Mall, Fretting behavior of Ti-6Al-4V under combined high cycle and low cycle fatigue loading. International Journal of Fatigue. 2001. 23

12.   H. Proudhon, S. Fouvry, Determination and prediction of the fretting crack initiation: introduction of the (P,Q,N) representation and definition of a variation process volume. International Journal of Fatigue. 2005

13.   M.P. Szolwinski, T.N. Farris, Observation, analysis and prediction of fretting fatigue in 2024-T351 alluminium alloy. WEAR. 1998. 221

14.   S. Fouvry, D. Nowell, K. Kubiak, D.A. Hills, Prediction of fretting crack propagation based on a short crack methodology. Engineering Fracture Mechanics. 2008. 75

15.   C.D. Lykins, S. Mall, V. Jain, An Evaluation of parameters for predicting fretting fatigue crack initiation. International Journal of Fatigue. 2000. 22

16.   J.J. Madge, S.B. Leen, P.H. Shipway, A combined wear and crack nucleation-propagation methodology for fretting fatigue prediction. International Journal of Fatigue. 2008. 30

17.   A. Hutson, S. Sathish, T. Nicholas, Progression of fretting fatigue damage in Ti-6Al-4V. Tribology international. 2006. 39

18.   A.L. Hutson, C. Nelsen, T. Nicholas, Characterization of fretting fatigue crack initiation processes in CR Ti-6Al-4V. Tribology international. 2003. 36

19.   P.D. Nicolaou, E.B. Shell, T.E. Matikas, Microstructural and surface characterization of Ti-6Al-4V alloys after fretting fatigue. Materials science & engineering. 1999. A269

20.   C.D. Lykins, S. Mall, V. Jain, Combined experimental-numerical investigation of fretting fatigue crack initiation. International Journal of Fatigue. 2001. 23

21.   Kubiak, K., Quantification de la fissuration d'un contact soumis à des sollicitations complexes en fretting wear et fretting fatigue. PhD manuscript. 2006

22.   L.J. Fellows, D. Nowell, D.A. Hills, On the initiation of fretting fatigue cracks. WEAR. 1997. 205

23.   Y. Kondo, C. Sakae, M. Kubota, K. Yanagihara, Non-propagating crack behaviour at giga-cycle fretting fatigue limit. Fatigue Fract Engng Mater Struct. 2004. 28

24.   M. Kubota, N. Noyama, C. Sakae, Y. Kondo, Fretting fatigue in hydrogen gas. Tribology international. 2006. 39

25. M. Kubota, Y. Tanaka, K. Kuwada, Y. Kondo, Mechanism of reduction of fretting fatigue limite in hydrogen gas environment. Proceedings of the 3rd International Conference on Material and Processin ICM&P 2008. 2008

26. M. Kubota, Y. Tanaka, Y Kondo, Fretting fatigue strenght of SCM435H steel and SUH660 heat-resistant steel in hydrogen gas environment. Tribotest. 2008. 14

27. Johnson, H.H., Calibrating the electrique potential method for studying slow crack growth. Materials Research & Standards. 1965. 5

28. international, ASTM, Standard test method for measurement of fatigue crack growth rates. ASTM E647-05. 2007

29. L. Gandossi, S.A. Summers, N.G. Taylor, R.C. Hurst, B.J. Hulm, J.D. Parker, The potential drop method for monitoring crack growth in real components subjected to combined fatigue and creep conditions: application of FE techniques for deriving calibration curves. Pressure Vessels and Piping. 2001. 78

30. M. Andersson, C. Persson, S. Melin, Experimental and numerical investigation of crack closure measurments with electrical potential drop technique. International Journal of Fatigue. 2006. 28

31. V. Spitas, C. Spitas, P. Michelis, Real-time measurement of shear fatigue crack propagation at high-temperature using the potential drop technique. Measurement. 2008. 41